

Composition dependence of structural evolution of Ni–Zr alloys during cooling

This article has been downloaded from IOPscience. Please scroll down to see the full text article.

2007 J. Phys.: Condens. Matter 19 086212

(<http://iopscience.iop.org/0953-8984/19/8/086212>)

View [the table of contents for this issue](#), or go to the [journal homepage](#) for more

Download details:

IP Address: 129.252.86.83

The article was downloaded on 28/05/2010 at 16:18

Please note that [terms and conditions apply](#).

Composition dependence of structural evolution of Ni–Zr alloys during cooling

QuanWen Yang and Tao Zhang¹

Department of Materials Science and Engineering, Beijing University of Aeronautics and Astronautics, Beijing 100083, People's Republic of China

E-mail: zhangtao@buaa.edu.cn

Received 31 July 2006, in final form 10 November 2006

Published 9 February 2007

Online at stacks.iop.org/JPhysCM/19/086212

Abstract

The solidification of binary alloys $\text{Ni}_x\text{Zr}_{100-x}$ ($x = 5.0, 10.0, 16.7, 33.3, 0.50, 66.7, 83.3, 90.0, 95.0$ at.%) at a cooling rate of $2.0 \times 10^{11} \text{ K s}^{-1}$ is studied with molecular dynamics simulation methods. The simulation results show that the number of icosahedral clusters with 13 atoms (Ih13) in these solidified $\text{Ni}_x\text{Zr}_{100-x}$ alloys at 300 K increases first and then decreases with increasing Ni concentrations, and reach a maximum at $x = 66.7$. Both the increasing rates of icosahedral pairs 1551 and 2331 and the decreasing rate of atomic diffusions during cooling in liquid $\text{Ni}_{66.7}\text{Zr}_{33.3}$ alloy are the largest among all those in the liquid Ni–Zr alloys simulated. It is the highest changing rates of icosahedral pairs that result in the highest glass-forming ability of the alloy $\text{Ni}_{66.7}\text{Zr}_{33.3}$. This illustrates that the structural evolutions of liquid alloys play a paramount role in determining the final structures of these solidified alloys, and further determine the glass-forming ability of alloys.

1. Introduction

Bulk amorphous alloys present important applications [1] because of their superior properties, such as unique thermal, chemical, mechanical and magnetic properties. Generally, typical reported bulk glassy alloys systems satisfy the three empirical rules proposed by Inoue *et al* [2], which are extensively used in designing new bulk metal glasses. Other criteria for evaluating the glass-forming ability (GFA) of alloys have also been proposed, such as the supercooled liquid region $\Delta T_x = T_x - T_g$, reduced glass transition temperature $T_{rg} = T_g/T_l$, and a dimensionless parameter $\gamma = T_x/(T_g + T_l)$ [3], where T_x is the onset crystallization temperature, T_g is the glass transition temperature, and T_l is the liquidus temperature. Because of the continuing lack of understanding of the mechanism of the GFA of alloys, a universal principle has not been established in developing new bulk metal glasses. Several empirical methods, such as

¹ Author to whom any correspondence should be addressed.

developing amorphous alloys with deep eutectic composition [4] or adopting the effective conduction electron per atom ratio (e/a) [5], have been proposed for designing alloys with high GFA. For finding a fundamental rule in developing new bulk metallic glasses (BMGs), it is paramount currently to understand the mechanism of the GFA.

The GFAs of alloys reflect the kinetic properties of alloys, and they are decided by the intrinsic properties of compositional elements and their interaction, which also decide the structural evolution of alloys. Therefore, the difference of their GFAs, as with many properties of alloys, can be reflected with the characteristics of structures. Frank hypothesized that undercooled metallic liquids contain a significant degree of icosahedral order [6], which was proved by Kelton *et al* [7] with direct experimental observation. The quasicrystalline phase presents a barrier for crystallizing of a melt, and will be retained in rapid solidified alloys, such as that observed in binary alloys $\text{Al}_{14}\text{Mn}_{86}$ [8], $\text{Zr}_{70}\text{Pd}_{30}$ [9], $\text{Zr}_{80}\text{Pt}_{20}$ [10], and other multicomponent amorphous alloys [11, 12]. The location rule of atomic distribution in the icosahedral clusters was studied by simulation [13] and experiment [14] recently which showed that the centre of the icosahedral cluster was mainly occupied by the smaller atom.

Holland-Moritz *et al* found that the activation threshold for nucleation was small for the icosahedral quasicrystalline phase by measurements of Al–Cu–Fe and Al–Cu–Co liquids, and they assumed that icosahedral short-range order prevails in the undercooled melt [15]. The icosahedral structure in a supercooled liquid gives rise to interfacial energy that depress the crystallization of the melt, so it is supposed that increased numbers of icosahedra enhance the GFA of binary or multicomponent alloys. Therefore, the icosahedra are one of the characteristic microstructures of the BMGs, and studying the icosahedral characteristics and their evolution during cooling is beneficial for understanding the mechanism of the GFA.

Because the GFA of alloys is sensitive to their compositions, one convenient way of studying the nature of it by structures is to investigate the compositional effect of the same alloy system. In this paper, we will present the composition dependence of the structural evolution of Ni–Zr alloys during cooling processes with molecular dynamics simulation techniques, and reveal what happens during the solidifying processes. The evolutions of icosahedral short-range order and atomic diffusion in Ni–Zr alloys are investigated to reveal the nature of the GFA.

2. Computer simulations

The present molecular dynamics simulations are carried out as isothermal–isobaric (N, P, T) calculations, in which the systems are coupled to a bath with constant temperature and constant pressure [16]. For the Ni–Zr alloy system with periodical boundary conditions, the Verlet velocity scheme [17] is implemented as a time integration algorithm with time step Δt equal to 2.5×10^{-15} s. To determine the interatomic forces of different atom pairs, the tight-binding potential of Ni–Zr alloys derived by Massobrio *et al* [18, 19] are introduced, in which the total potential energy of the system is given by

$$E = \sum_{i=1}^N \left[\sum_{j=1 \neq i}^N A_{\alpha\beta} \exp \left[-p_{\alpha\beta} \left[\frac{r_{ij}^{\alpha\beta}}{d_{\alpha\beta}} - 1 \right] \right] - \left\{ \sum_{j=1 \neq i}^N \xi_{\alpha\beta}^2 \exp \left[-2q_{\alpha\beta} \left[\frac{r_{ij}^{\alpha\beta}}{d_{\alpha\beta}} - 1 \right] \right] \right\}^{1/2} \right],$$

where $r_{ij}^{\alpha\beta} = |r_i^\alpha - r_j^\beta|$, and N is the total number of Ni and Zr atoms. The parameters $p_{\alpha\beta}$, $q_{\alpha\beta}$, $A_{\alpha\beta}$, $\xi_{\alpha\beta}$ for different pairs are provided in [18, 19]. Interactions of atoms have been computed within a spherical cutoff radius $r_c = 0.53$ nm as in [19].

By molecular dynamics simulations, we first construct $\text{Ni}_x\text{Zr}_{100-x}$ ($x = 0, 5.0, 10.0, 16.7, 33.3, 50.0, 66.7, 83.3, 90.0, 95.0, 100$ at.%) alloy systems of 2048 atoms with an arbitrary structure, and run them at 2500 K, which is higher than the melting points of Ni (1728 K) and

Zr (2125 K), for 1.0×10^5 time steps to reach an equilibrium liquid state, and then run them at a cooling rate of $2.0 \times 10^{11} \text{ K s}^{-1}$ (the temperature decreases 5 K every 10 000 steps) to obtain crystalline or amorphous Ni–Zr alloys at 300 K. The simulations of single Ni ($x = 100$) and Zr ($x = 0$) were performed for comparison. The structures of a binary alloy are a function of both the composition and the quench rate. In this paper, our aim is to reveal the composition effect on the structural evolution during cooling, and therefore a uniform quench rate is adopted in the simulations. It should be noted that the cooling rate employed in the simulations is very much larger than can be achieved in reality. Although it is difficult to observe the simulation results at such a large quench rate by experiment, the physical process at atomic scale can be described in detail by the simulations.

To identify icosahedral clusters in Ni–Zr amorphous alloys, we employ the Honeycutt–Andersen (HA) pair analysis technique [20]. If two atoms are within a given separating distance, chosen to equal the position of the first minimum in the corresponding pair correlation functions, they are said to form a bond. The first index is 1 if the pair is bonded and 2 otherwise. The number of common atoms bonded with the two atoms is recorded as the second index. The third index indicates the bond number between the common atoms, and the fourth index is used to distinguish the arrangement of bond. The separating distances of Ni–Ni, Ni–Zr and Zr–Zr decided by the adopted interatomic potential are 0.32, 0.37 and 0.42 nm, respectively [18]. With the HA bond pair analysis technique, the face-centred cubic (fcc) structure is characterized by pair 1421, the hexagonal closed-packed (hcp) structure is characterized by pair 1422, and the body-centre cubic (bcc) is characterized by pair 1441 and pair 1661, while large numbers of pairs 1551 and 2331 existing in liquid and glass are characteristic of an icosahedron. The smallest icosahedral cluster Ih13 is composed of 13 atoms, with the centre one surrounded by 12 vertex atoms. For the case that the centre atom of Ih13 forms a bond pair 1551 with every one of its nearest neighbours according to the HA bond pair analysis technique, it is convenient to confirm these Ih13 in the amorphous alloys systems.

It is reasonable to evaluate the crystallizing degree for solidified alloys with the relative crystalline or non-crystalline characterized bond pairs. In this paper, we will estimate the GFA of alloys by those non-crystalline characterized bond pairs, mainly by pairs 1551 and 2331, and the number of Ih13 clusters in the alloys. That is to say, alloys with larger number of non-crystalline characterized bond pairs or icosahedral clusters are said to possess higher GFA.

3. Results and discussion

3.1. Configurations of Ih13 clusters in solidified alloys at 300 K

The structures of the Ni–Zr alloys obtained at the cooling rate of $2.0 \times 10^{11} \text{ K s}^{-1}$ depend strongly on their compositions. The atomic configurations of the solidified $\text{Ni}_x\text{Zr}_{100-x}$ alloys at 300 K are shown in figure 1. It can be seen from figure 1 that the $\text{Ni}_x\text{Zr}_{100-x}$ alloys with $x = 5.0, 10.0, 95.0$ respectively are crystalline or partially crystalline, while the remaining alloys ($x = 16.7, 33.3, 0.50, 66.7, 83.3, 90.0$ respectively) are amorphous. These configurations also show that the numbers of Ih13 clusters in these alloys depend on the compositions. As shown in figure 2, the number of Ih13 clusters in $\text{Ni}_x\text{Zr}_{100-x}$ alloys increases first and then decreases with concentration of Ni ($x = 16.7-95.0$). We confirm that $\text{Ni}_{66.7}\text{Zr}_{33.3}$ presents the highest GFA for the richest number of Ih13 clusters existing in it. There are no Ih13 clusters for the alloy $\text{Ni}_{10}\text{Zr}_{90}$, while a few Ih13 clusters exist in the alloy $\text{Ni}_{95}\text{Zr}_5$. This illustrates that the Ni–Zr alloy with 5% Zr presents the better icosahedral cluster forming ability than the Ni–Zr alloy with 10% Ni. That is to say, the Zr element presents the better function in enhancing the GFA, which concurs well with the fact that many Zr-based BMGs have been fabricated.

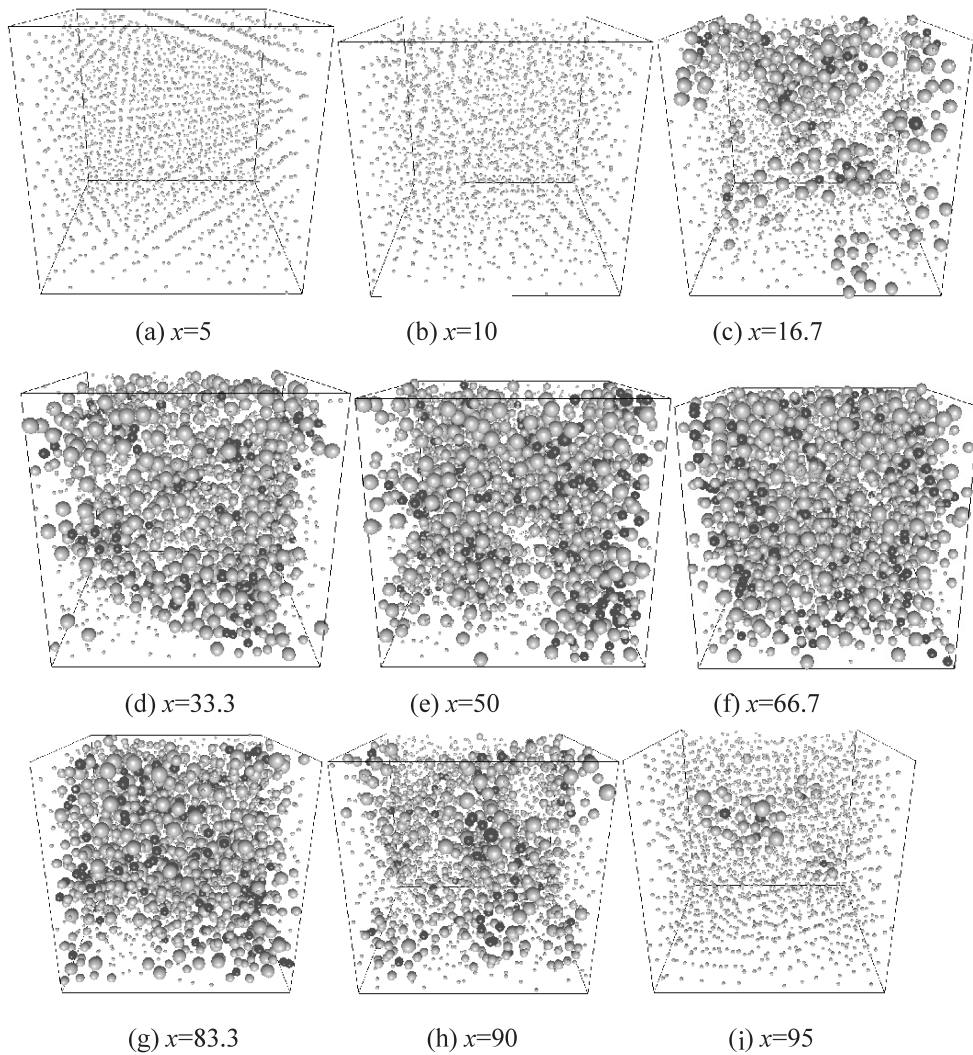


Figure 1. Configurations of Ih13 clusters in $\text{Ni}_x\text{Zr}_{100-x}$ alloys with 2048 atoms at 300 K, with black spheres representing the centre atoms of Ih13 clusters, grey spheres representing the vertex atoms of Ih13 clusters, and spheres of the smallest size representing atoms not belonging to Ih13 clusters. The largest spheres and those of middle size represent Zr atoms and Ni atoms of Ih13 clusters, respectively.

The regular variation of the number of Ih13 clusters reflects the composition dependence of the GFA of alloys, so that it is necessary to investigate their growth during cooling.

3.2. Growth of Ih13 clusters during cooling

The numbers of Ih13 clusters in Ni–Zr alloys as a function of temperature are presented in figure 3. The curves are shown in two groups, with $x = 66.7$ being the partition for convenient comparisons. The curves in figures 4 and 5 are shown in the same style. To reduce the fluctuation of the curves, the numbers of Ih13 clusters (in figure 3) or the values of bond pairs (in figure 4) have been averaged over ten configurations in the last 1000 simulation steps at every temperature in the simulations.

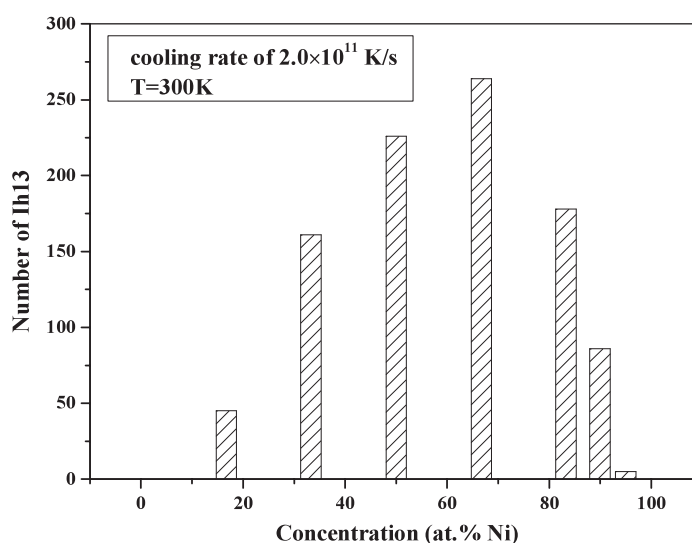


Figure 2. Numbers of Ih13 clusters in the solidified $\text{Ni}_x\text{Zr}_{100-x}$ alloys at 300 K.

For $\text{Ni}_x\text{Zr}_{100-x}$ alloys with $x = 16.7, 33.3, 50.0, 66.7, 83.3, 90.0$, respectively, the number of Ih13 clusters increases with decreasing temperature during the cooling processes, while that of the $\text{Ni}_x\text{Zr}_{100-x}$ alloys with $x = 0, 5.0, 10.0, 100$, respectively, increases with decreasing temperatures first and then drops quickly at their crystallizing temperatures. The $\text{Ni}_{95.0}\text{Zr}_{5.0}$ alloy is an exception in that a few Ih13 clusters are retained in it at lower temperatures, though most atoms in it have crystallized. At higher temperatures ($T > 1200$ K), small numbers of Ih13 clusters are found in these Ni–Zr alloys. At lower temperatures ($T < 1200$ K), the growth rates of Ih13 clusters increase first (for $x < 66.7$) and then decrease (for $x > 66.7$) with increasing Ni concentration x during solidification; the $\text{Ni}_{66.7}\text{Zr}_{33.3}$ alloy has the maximum number. This illustrates that the growth rates of Ih13 clusters in $\text{Ni}_x\text{Zr}_{100-x}$ alloys are dependent on their compositions. The largest number of Ih13 clusters existing in the solidified $\text{Ni}_{66.7}\text{Zr}_{33.3}$ alloy is achieved by its largest increase during solidification.

3.3. Bond pair analysis

Because the pairs 1551 and 2331 characterize the icosahedron, they can be identified as the kernel of an icosahedral cluster in liquid alloys. The existence of these pairs in a supercooled liquid can reduce the number of other pairs characterizing crystalline structures and depress the crystallization of the melt. Therefore, the evolution of pairs 1551 and 2331 plays a paramount role in describing the GFA of alloys. As shown in figure 4, the composition dependence of pairs 1551 and 2331 in Ni–Zr alloys at low temperatures ($T < 1100$ K) is observed with the same trend as that of Ih13 clusters. What differs from Ih13 clusters is that these pairs also present a composition dependence at higher temperatures ($T > 1100$ K).

It can be seen from figure 4 that the numbers of both 1551 and 2331 pairs in a liquid alloy decrease with increasing Ni concentrations x at a given temperature ($T > 1100$ K). This indicates that Zr atoms are more apt to form five-fold symmetry structures than Ni atoms in the liquid state. Although there are lots of 1551 pairs at high temperatures, almost no Ih13 clusters are found in these alloys (see figure 3). This indicates that the Ih13 cluster is very unstable in high-temperature liquid alloys.

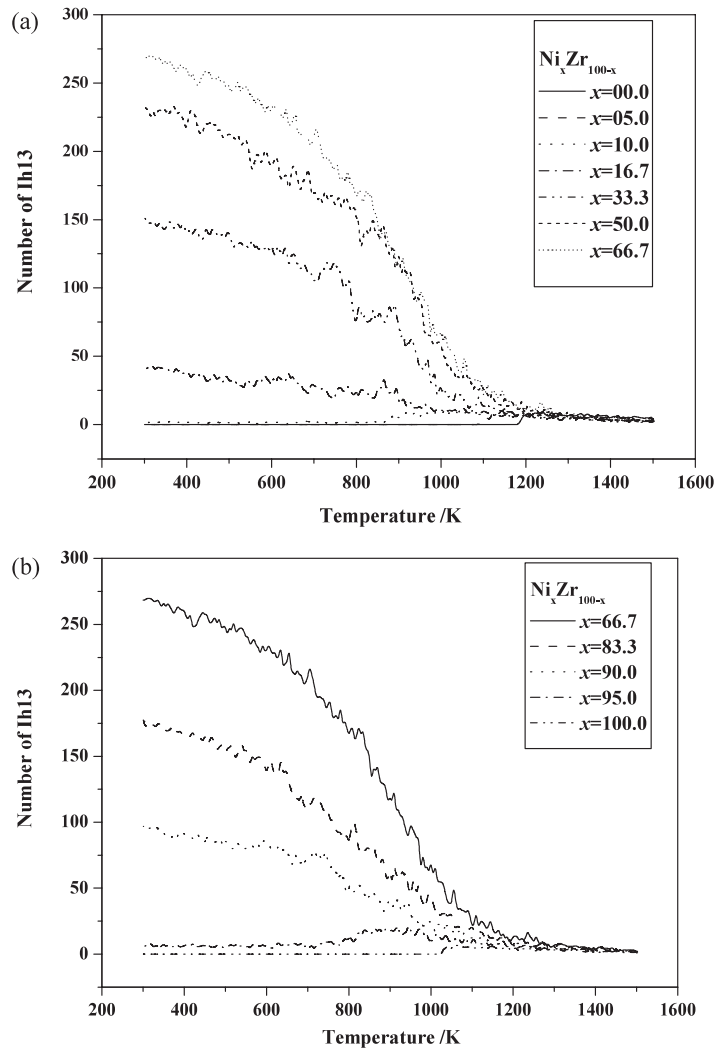


Figure 3. Numbers of Ih13 clusters in $\text{Ni}_x\text{Zr}_{100-x}$ alloys as a function of temperature during cooling at a rate of $2.0 \times 10^{11} \text{ K s}^{-1}$ (short-dotted curve in (a) versus solid curve in (b) for $x = 66.7$).

The growth rates of the icosahedral pairs increase first and then decrease with increasing x during cooling, with the maximum appearing at $x = 66.7$. As $x < 66.7$, the curves of bond pairs 1551 or 2331 intersect each other at about 1100 K (assuming that there is no crystallization for these alloys with $x = 0.0, 5.0, 100$); therefore, the $\text{Ni}_x\text{Zr}_{100-x}$ alloys with the smaller x have more 1551 and 2331 bond pairs above 1100 K and have fewer below 1100 K. As $x > 66.7$, the $\text{Ni}_x\text{Zr}_{100-x}$ alloys with smaller x always have the larger numbers of the bond pairs 1551 and 2331 at any temperature. Therefore, the numbers of 1551 and 2331 pairs in $\text{Ni}_{66.7}\text{Zr}_{33.3}$ are not the most at any temperature, and the largest numbers of these icosahedral pairs found in solidified $\text{Ni}_{66.7}\text{Zr}_{33.3}$ alloy are achieved by their largest growth rates during cooling.

The simulation results are different from that of Andersen's molecular dynamics simulation of a Lennard-Jones liquid [21], which indicated that the inherent structures showed no significant changing at high temperatures and the 1551 and 2331 pairs only increased

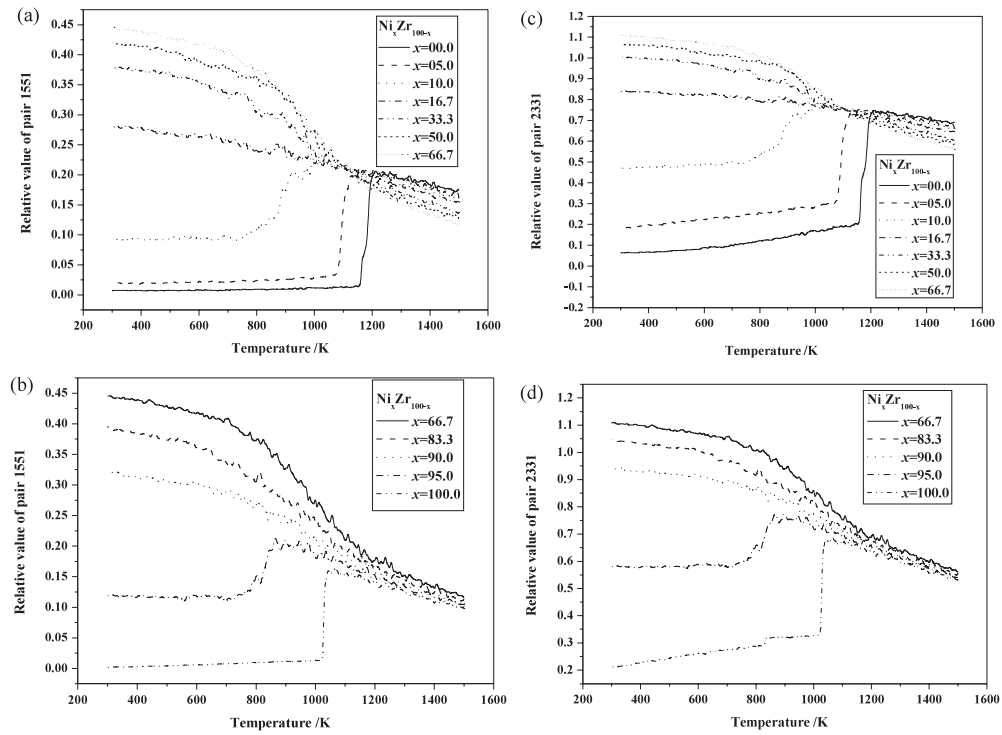


Figure 4. Change in bond pairs 1551 and 2331 of $\text{Ni}_x\text{Zr}_{100-x}$ alloys with temperature during cooling at a rate of $2.0 \times 10^{11} \text{ K s}^{-1}$ (short-dotted curves in (a) and (c) versus solid curve in (b) and (d) for $x = 66.7$, respectively).

with decreasing temperatures at lower temperatures. The inherent structures achieving local potential-energy minima were obtained with steepest-descent paths [22]. The difference indicates that the inherent structures of a liquid cannot be observed with kinetic processes.

3.4. Diffusions in Ni–Zr alloys during cooling

To identify the effects of icosahedral pairs on the dynamic behaviour of supercooled liquids, we record the mean square displacements (MSDs) of atoms in Ni–Zr alloys during the last 2.5 ps at every temperature in the simulations. It can be seen from figure 5 that the diffusions of atoms in the alloys increase first and then decrease with increasing x at high temperatures ($T > 1200 \text{ K}$), with that of $\text{Ni}_{66.7}\text{Zr}_{33.3}$ reaching the maximum. The variations of activities with compositions are different from that of icosahedral pairs, which decrease with x at higher temperatures (see figure 4). This illustrates that the atomic diffusions of alloy are independent of the numbers of icosahedral pairs and cannot be depressed by these pairs in high-temperature liquid alloys.

The slow variations of atomic diffusions are observed near about 1000 K; the range can be identified as the glass transition region. Corresponding to the largest increasing rate of icosahedral pairs, the atomic diffusions of the alloy with $x = 66.7$ present the largest descending rate during cooling, which results in its lowest atomic diffusion at the glass transition region. The depressed atomic diffusion implies the enhancing of the alloy's viscosity, so that the lowest atomic diffusion can also manifest the highest GFA of $\text{Ni}_{66.7}\text{Zr}_{33.3}$. We

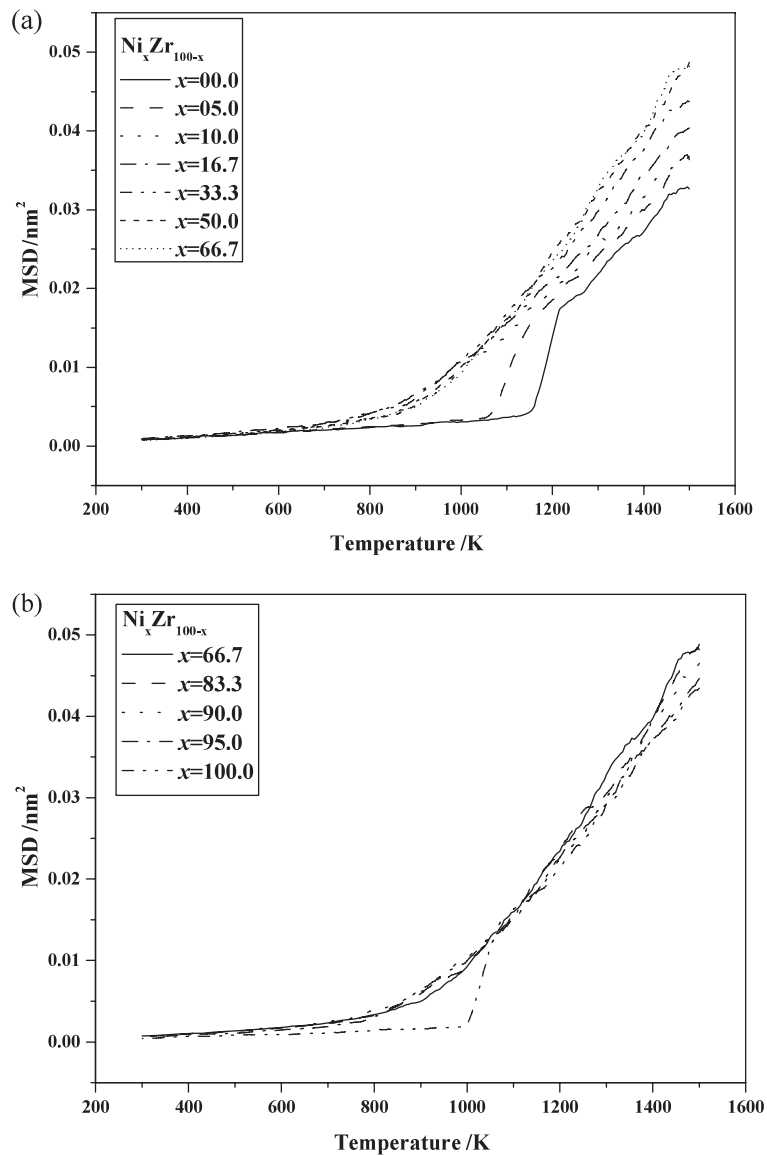


Figure 5. The mean-square displacements of atoms in Ni–Zr alloys as a function of temperature during cooling at a rate of $2.0 \times 10^{11} \text{ K s}^{-1}$ (short-dotted curves in (a) versus solid curve in (b) for $x = 66.7$).

conclude that the rapid increasing viscosity of alloys with high GFA is induced by the fast growth rates of icosahedral pairs in them.

We are sure that the quench rate effect exists in our simulations and that any Ni–Zr alloy will crystallize at sufficiently low quench rate. This indicates especially that the structures observed in the simulations are kinetically trapped and not thermodynamically favourable for lower cooling rates. Because many BMGs have been fabricated by rapid solidification, it is necessary to investigate the solidifying process of these alloys at high quench rates. We contend that similar structural evolution trends should be observed at a lower quench rate for the same

alloy system, so that the structure signature of alloys in the rapid solidification can be reflected sufficiently in our simulations.

At a higher temperature, the atoms in the liquid alloys have enough kinetic energy to drive the system into equilibrium states, and the atoms can adjust their configurations in time to minimize the system's free energy even at fast quench rates. The structural evolutions of liquid alloys at higher temperatures can be understood as the reflection of the characteristics of structures moving on the hypersurfaces of minimum free energies. The systems' free energies are determined by the intrinsic physical properties of elements and their interactions, so are the compositions at the maximum. That is to say, the largest growth rates of icosahedral pairs at $x = 66.7$ in our simulations are brought by the atomic interactions of Ni–Ni, Ni–Zr and Zr–Zr.

We think that the alloys' compositions reaching the maximum changing rates of icosahedral pairs differ from each other for different alloy systems, but the trend of the GFA with composition is generic. It can be seen from the simulation results that if a pure Ni or Zr alloy is added with another element, the growth rate of icosahedral pairs will increase. This indicates that it is the combination of two elements that leads to the faster growth rates of icosahedral pairs in alloys. When the alloy's composition deviates from that at the maximum, the quantities of crystalline pairs must increase and promote the crystallizing of alloy. The more deviation from that at the maximum will bring the more crystalline pairs in alloy; therefore, there must be only one peak in glass formation tendency with compositions.

The simulation results show that both the GFA and the viscosity of the liquid alloy below glass transition temperatures are determined by the growth rates of icosahedral structures in high-temperature liquid alloys; therefore, the nature of an alloy's GFA can also be illuminated by the characteristics of structural evolutions on the hypersurfaces of minimum free energies. As a thermodynamic characteristic, the variations of icosahedral pairs in equilibrium liquid alloys can elucidate the sharp rise of viscosity of alloy during glass transition, which is the kinetic quality of alloys. This indicates that the kinetic properties of alloys in rapid solidification are related qualitatively to thermodynamical properties, and suggest a new way to study the kinetic behaviour in glass transitions by thermodynamic qualities.

4. Conclusions

A composition dependence of icosahedral clusters was found in solidified Ni–Zr alloys by molecular dynamics simulations. The largest number of icosahedral clusters and their characterizing 1551 and 2331 pairs existing in the $\text{Ni}_{66.7}\text{Zr}_{33.3}$ alloy are brought about by their largest growth rates during cooling. The larger increasing rate of the icosahedral pairs also results in depressed atomic diffusions in the glass transition region. The GFA of alloys can be described by the evolution of icosahedral pairs in liquid alloys, which indicates that the kinetic properties of alloys in rapid solidification are related qualitatively to the thermodynamical properties.

Acknowledgments

This work was financially supported by the National Natural Science Foundation of China (Nos 50225103 and 50631010) and PCSIRT (IRT 0512).

References

- [1] Inoue A and Takeuchi A 2002 *Mater. Trans.* **43** 1892
- [2] Inoue A 1995 *Mater. Trans. JIM* **36** 866
- [3] Lu Z P and Liu C T 2002 *Acta Mater.* **50** 3501

- [4] Turnbull D 1969 *Contemp. Phys.* **10** 473
- [5] Wang Y M *et al* 2003 *Scr. Mater.* **48** 1525
- [6] Frank F C 1952 *Proc. R. Soc. A* **215** 43
- [7] Kelton K F *et al* 2003 *Phys. Rev. Lett.* **90** 195504
- [8] Shechtman D, Blech I, Gratias D and Cahn J W 1984 *Phys. Rev. Lett.* **53** 1951
- [9] Murty B S, Ping D H and Hono K 2000 *Scr. Mater.* **43** 103
- [10] Saida J, Matsushita M and Inoue A 2000 *Appl. Phys. Lett.* **77** 73
- [11] Inoue A *et al* 1999 *Mater. Trans. JIM* **40** 1181
- [12] Saida J, Matsushita M and Inoue A 2001 *Phil. Mag. Lett.* **81** 39
- [13] Yang Q W and Zhang T 2006 *Chin. Phys. Lett.* **23** 915
- [14] Yang L *et al* 2006 *Appl. Phys. Lett.* **88** 241913
- [15] Holland-Moritz D *et al* 1998 *Acta Mater.* **46** 1601
- [16] Berendsen H J C *et al* 1984 *J. Chem. Phys.* **81** 3684
- [17] Allen M P and Tildesley D J 1987 *Computer Simulation of Liquids* (Oxford: Clarendon)
- [18] Massobrio C, Pontikis V and Martin G 1989 *Phys. Rev. Lett.* **62** 1142
- [19] Massobrio C, Pontikis V and Martin G 1989 *Phys. Rev. B* **41** 10486
- [20] Honeycutt J D and Andersen H C 1987 *J. Phys. Chem.* **91** 4950
- [21] Jonsson H and Andersen H C 1988 *Phys. Rev. Lett.* **60** 2295
- [22] Stillinger F H and Weber T A 1982 *Phys. Rev. A* **25** 978